BIOCHEMICAL PHARMACOLOGY 76 (2008) 268–278

available at www.sciencedirect.com

ScienceDirect

journal homepage: www.elsevier.com/locate/biochempharm

Differential regulation of human hepatic flavin containing monooxygenase 3 (*FMO3*) by CCAAT/enhancer-binding protein β (C/EBPβ) liver inhibitory and liver activating proteins

David E. Klick, Jeff D. Shadley, Ronald N. Hines *

Departments of Pediatrics and Pharmacology and Toxicology and The Children's Research Institute, Medical College of Wisconsin and Children's Hospital and Health System, Milwaukee, WI 53226, USA

ARTICLE INFO

Article history:
Received 31 March 2008
Accepted 1 May 2008

Keywords:
Flavin-containing monooxygenase
FMO3
Gene regulation
CCAAT/enhancer-binding protein
HepG2 cells

ABSTRACT

Flavin-containing monooxygenase 3 (FMO3) is important for oxidative xenobiotic metabolism, but regulation of the *FMO3* gene remains poorly understood. *FMO3* is not expressed in HepG2 cells, a commonly employed model for hepatic gene regulation studies. Transcription factor transient expression and treatment with histone deacetylase or DNA methylase inhibitors identified decreased hepatic nuclear factor (HNF) 4α levels and DNA hypermethylation as mechanisms suppressing HepG2 *FMO3* expression. The absence of major deficiencies in transcriptional machinery suggested that within limits, the HepG2 model is suitable for the study of *FMO3* regulation. DNA–protein binding studies with HepG2 cell and hepatic tissue nuclear protein extracts and reporter construct transient expression experiments were performed to characterize *FMO3* sequences from position −494 to −439 (domain I), previously demonstrated to significantly impact promoter function. Although both HNF3β and CCAAT enhancer-binding protein (C/EBP) were observed to specifically interact with this element using HepG2 cell nuclear proteins, only C/EBP DNA–protein interactions were observed using adult liver nuclear proteins. No specific DNA/protein interactions were observed using fetal liver nuclear proteins. Mutation of a putative HNF3β element had no effect on *FMO3* promoter activity, while mutagenesis of a distinct, but overlapping C/EBP element resulted in a 55% reduction in activity. Furthermore, promoter activity was regulated as a function of defined C/EBPβ liver activating protein:liver inhibitory protein ratios through this same element. Chromatin immunoprecipitation demonstrated C/EBPβ binding to the *FMO3* domain I element in intact cells and adult liver tissue. These results are consistent with C/EBPβ being important for regulating hepatic *FMO3* expression.

1. Introduction

The flavin-containing monooxygenases (FMOs) are highly versatile enzymes important for the oxidative metabolism of numerous compounds containing soft nucleophilic heteroatoms, *i.e.*, nitrogen, sulfur, selenium, and phosphorous. Substrates include 1–2% of clinically important drugs [1], *e.g.*, tamoxifen, itopride, benzydamine, olopatidine, xanomeline,

* *Corresponding author at*: Medical College of Wisconsin, TBRC/CRI/CPPT, 8701 Watertown Plank Rd., Milwaukee, WI 53226, USA. Tel.: +1 414 955 4322; fax: +1 414 955 6651.
E-mail address: rhines@mcw.edu (R.N. Hines).
0006-2952/$ – see front matter
doi:10.1016/j.bcp.2008.05.002

and sulindac. Toxicant/pesticide substrates include nicotine, aldicarb, fenthion, and fonofos [2]. The FMO's broad substrate specificity has been attributed to a unique catalytic mechanism in which the enzyme is pre-activated in the presence of oxygen and NADPH, but in the absence of substrate, resulting in specificity by exclusion [3]. There are 11 members of the human *FMO* gene family encoded on the long arm of chromosome 1 [4]. *FMO1-5* encode functional proteins and display distinct temporal-, tissue-, and species-specific expression patterns [5], while *FMO6P-11P* are pseudogenes [4,6].

FMO3 is the major human adult liver FMO, however expression is absent in the fetus and most neonates. Expression is detectable in most individuals between the ages of 1 and 12 months. Hepatic FMO3 is present at intermediate levels between one and 11 years of age. With the onset of puberty, enzyme levels increase in a gender-independent fashion, approaching adult levels by 18 years of age [7]. In the adult liver, FMO3 constitutes one of the major oxidative microsomal enzymes exhibiting expression levels similar to CYP2C9 [7–9]. However, FMO3 also exhibits a species-specific expression pattern [5,10,11].

Although the overall FMO3 expression pattern has been well characterized, little is known regarding regulatory mechanisms. Consistent with the pronounced temporal- and tissue-specific differences in FMO3 mRNA, protein, and activity, transcription is hypothesized to be a major point of regulation [7,9,12]. Thus, temporal- and tissue-specific transcription factors are likely primary regulators of human *FMO3* constitutive and developmental expression. In a previous study from this laboratory, *FMO3* promoter domains within 3000-bps of the transcription site were characterized [13]. Based on an initial assessment, subsequent studies focused on the first 500 bps of the *FMO3* promoter as domains within this region accounted for a 20-fold increase in expression over that observed with the basal promoter versus minimal changes mediated by domains further upstream. A number of important regulatory elements between position −386 and +1 were identified (Fig. 1). These included nuclear factor Y (NFY), pre-B-cell leukemia factor 2/homeobox binding protein heterodimer (Pbx_2/Hox), upstream stimulatory factor-1 (USF-1), an unidentified GC box binding protein, and yin yang 1 (YY1) responsive elements. The goal of the current study was to explore mechanisms whereby *FMO3* is repressed in HepG2 cells and to further characterize the molecular factors contributing to human *FMO3* regulation. The latter studies specifically focused on a previously identified, but uninvestigated more distal positive regulatory domain I (*FMO3* position −494 to −439) which was associated with a 3-fold increase in promoter activity.

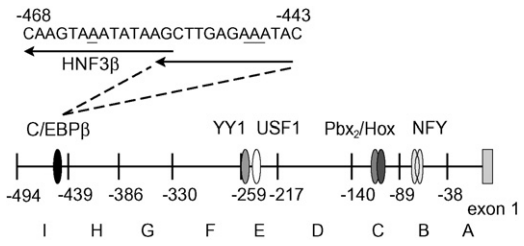

Fig. 1 – Human *FMO3* regulatory elements. A schematic is presented showing putative *FMO3* regulatory domains identified by deletion analysis of *FMO3*/luciferase reporter constructs (domains A–I) and specific transcription factor responsive elements identified by DNA–protein binding reactions and site-directed mutagenesis of *FMO3* reporter constructs [13]. The putative C/EBPβ and HNF3β domain I sites that are the focus of the current study also are shown. Underlined bases are those altered by site-directed mutagenesis which eliminated specific transcription factor binding.

2. Materials and methods

2.1. *Plasmid constructs and site-directed mutagenesis*

FMO3 coordinates are based on the GenBank reference assembly, NT_004487.18 GI:88943682, build 36.2 and a search of the DBTSS database (http://elmo.ims.u-tokyo.ac.jp/dbtss), which mapped a single transcription start site 1774-bps upstream of the exon 2 ATG start codon. Construction of the pRNH694 reporter construct (*FMO3* position −2952 to +42 directing luciferase expression) was previously described [13]. Site-directed mutagenesis of putative *FMO3* transcription factor binding sites within pRNH694 was performed using the QuikChange II XL Site-Directed Mutagenesis Kit (Stratagene, La Jolla, CA) as directed by the manufacturer. All mutations were verified by DNA sequence analysis and tested by electrophoretic mobility shift assay (EMSA) to ensure specific DNA–protein binding was eliminated without introduction of a false protein binding element.

The pcDNA3-HNF3β expression vector [14] was provided by Dr. Graeme Bell (University of Chicago, Chicago, IL). Full-length human cDNAs for hepatic nuclear factor (HNF) 4α, CCAAT/enhancer-binding protein (C/EBP) α, C/EBPβ liver activating protein (LAP), C/EBPβ liver inhibitory protein (LIP) and C/EBPδ were generated using polymerase chain reaction (PCR) DNA amplification, gene specific primers (see supplemental Table 1S) (Integrated DNA Technologies, Coralville, IA), and a human adult liver cDNA library as a template. The latter was prepared from total human adult liver RNA (Stratagene, La Jolla, CA) with the MonsterScript 1st-strand cDNA synthesis Kit (Epicentre Biotechnologies, Madison, WI). cDNAs were cloned into the pBJ5 expression vector [15].

2.2. *Electrophoretic mobility shift assays (EMSA)*

Six human fetal liver tissue samples (all first trimester) were obtained from the University of Washington Central Laboratory for Embryology Research, Seattle, WA. Three human adult liver tissue samples (from a 22-year-old white male, a 50-year-old white female, and a 68-year-old white female) were obtained from the Liver Tissue Procurement and Distribution System (Dr. Stephen Strom, University of Pittsburgh, Pittsburgh, PA). Fetal and adult liver tissue and HepG2 cell nuclear protein extracts were prepared using the NE-PER Nuclear and Cytoplasmic Extraction Reagent Kit (Pierce, Rockford, IL) following the manufacturer's protocol. EMSAs were performed as described by Klick et al. [13]. Antibodies for EMSA supershift experiments, HNF3β (M-20), C/EBPα (C-18), C/EBPβ

(H-7), C/EBPγ (C-20), and C/EBPδ (C-22), were obtained from Santa Cruz Biotechnology (Santa Cruz, CA). Double-stranded oligonucleotide consensus elements used in competitive EMSA included: HNF3 (5′-AAT TCA AGT CCA GGA CTT GTT TGT TCA GGA-3′) and C/EBP (5′-AGC TTG CAG ATT GCG CAA TCT GCA-3′) [16].

2.3. Cell culture and transient transfection

Normal human primary hepatocytes (15 months old male) were obtained from the Liver Tissue Procurement and Distribution System (Dr. Stephen Strom, University of Pittsburgh, Pittsburgh, PA) and cultured as previously described [17] prior to use in chromatin immunoprecipitation experiments. The HepG2 human hepatoblastoma cell line [18], a gift from Dr. Barbara Knowles (Jackson Laboratories, Bar Harbor, ME), was cultured and transfected as described by Luo et al. [19].

HepG2 cells were treated with trichostatin A (Sigma–Aldrich, St. Louis, MO) for 24 h to alter histone acetylation or 5-aza-2′-deoxycytidine (Sigma–Aldrich, St. Louis, MO) for 96 h with daily media/drug replacement to alter DNA methylation. After treatment, RNA was isolated with the Aurum Total RNA Mini Kit (BioRad, Hercules, CA). Glyceraldehyde-3-phosphate dehydrogenase (GAPDH) normalized FMO3 mRNA levels were determined by quantitative real-time PCR DNA amplification using the iScript One-Step reverse transcriptase coupled PCR (RT-PCR) Kit with SYBR Green, the iCycler iQ system (BioRad, Hercules, CA) and FMO3 forward 5′-TGG CCC TTG TAG TCC CTA CCA G-3′ and reverse 5′-GGC TTC TGA AGT CTC CCG ACC-3′, or GAPDH forward 5′-TGA AGC AGG CGT CGG AGG-3′ and reverse 5′-GCT TGA CAA AGT GGT CGT TGA GG-3′ primers (Integrated DNA Technologies, Coralville, IA). RT-PCR was performed using the following protocol: initial denaturation at 95 °C for 3 min, followed by 45 cycles consisting of denaturation at 95 °C for 0.10 min, annealing at 60 °C for 0.30 min, and extension at 72 °C for 1.0 min. Amplification was immediately followed by a DNA melting protocol: 1.0 min at 95 °C, 1.0 min at 55 °C, followed by 79 additional 1.0 min cycles increasing 0.5 °C in each successive cycle. Calculations of relative FMO3 mRNA concentrations were made using the comparative method as described by Bookout et al. [20].

2.4. Chromatin immunoprecipitation (ChIP)

Normal human primary hepatocytes were fixed with 1% formaldehyde and isolated chromatin fragmented as described by Shadley et al. [17]. Pooled frozen liver tissue from the three adult donors was pulverized in liquid nitrogen and fixed using a ratio of 0.1 g of tissue to 10 ml of fixing solution. After isolation, chromatin samples from tissue were treated with the Enzymatic Digestion kit (Active Motif, Carlsbad, CA) as directed by the manufacturer rather than fragmenting by sonication. Either preparation resulted in the majority of DNA molecules being between 100 and 650 bps in length. The ChIP assay was performed using the ChIP-It Express kit (Active Motif, Carlsbad, CA) with 2.5 μg of either C/EBPβ (C-19) antibody or rabbit preimmune IgG (Santa Cruz Biotechnology, Santa Cruz, CA). Isolated immunoprecipitated and input DNA were used as templates in quantitative PCR reactions (4–6 replicates/template) using the iQ SYBR Green Supermix (BioRad, Hercules, CA) as directed by the manufacturer. All amplification primers were obtained from Integrated DNA Technologies (Coralville, IA). Forward, 5′-TTA CCT GGT TCC TGG TAC-3′ (*FMO3* position −544 to −527), and reverse, 5′-AGC CCA ATA AGG AGG ATG-3′ (*FMO3* position −385 to −368), primers were used to amplify a 177 bp product that included the putative C/EBP element. Albumin [21] and *CYP3A4* [22] C/EBPβ elements were tested in parallel as positive controls using the following primers: albumin forward, 5′-TGA CAA GGT CTT GTG GAG AAA AC-3′, and reverse, 5′-AGG ACA AAC GGA GGG AAA TTA G-3′ and *CYP3A4* forward, 5′-CAG GGT CAG GCA AAA CAA G-3′, and reverse, 5′-TTC AGC AGA AAG GCA AAT GT-3′ which amplify 195 and 224-bp products, respectively. As negative controls, a 135-bp *FMO3* exon 9 fragment was included in the analysis: forward, 5′-TGG CCC TTG TAG TCC CTA CCA G-3′ and reverse, 5′-GGC TTC TGA AGT CTC CCG ACC-3′, as was a 174-bp fragment representing a sequence between the *GAPDH* and the *CNAP1* genes and generated using the control primers included in the Active Motif (Carlsbad, CA) ChIP-It express kit. The criteria of Aparicio et al. [23] were used to determine the suitability of data for inclusion in the analyses and to calculate binding differences as previously described [17]. The coefficient of variation using the non-selective precipitated template (IgG) was less than 5%.

2.5. Bisulfite sequencing of FMO3 promoter CpG sites

FMO3 CpG islands were identified using MethPrimer [24], which also was used to design primers for sequence analysis (see supplemental Table 1S). HepG2 cell and human adult and fetal liver genomic DNA were isolated as described by Koukouritaki et al. [25]. The EZ DNA Methylation-Gold Kit (Zymo Research, Orange, CA) was used as instructed by the manufacturer. The bisulfite-modified DNA was amplified using *FMO3* specific primers (see supplemental Table 1S) and sequenced to determine the methylation state of cytosine bases.

2.6. Sequence and data analysis

Selected sequences were scanned for potential transcription factor recognition sequences using the Match Program and the TRANSFAC Professional V11.1 database (BIOBASE Corporation, Wolfenbuettel, Germany) [26,27]. In each case, the Liver-Specific Matrix Profile was used with a minimum matrix similarity score of 0.7 and a core minimum similarity score of 0.75.

FMO3 gene sequences from various organisms were aligned using an exhaustive pairwise global alignment algorithm and progressive assembly using Neighbor-Joining phylogeny with default parameters (Clone Manager Professional Suite V8, Scientific & Educational Software, Cary, NC).

After correcting for transfection efficiency, transient expression data were compared using a one-way ANOVA with a Tukey post hoc test, while FMO3 mRNA levels were compared using either the Student's *t*-test or one-way ANOVA with a Holm-Sidak post hoc test (Sigma-stat version 3.11, Systat Software, San Jose, CA). ChIP quantitative PCR C_T

differences were compared using an unpaired *t*-test with Welch correction (Instat version 3.05, GraphPad Software, San Diego, CA). In all cases, *P*-values less than 0.05 were accepted as significant.

3. Results

3.1. *Endogenous FMO3 expression in HepG2 cells*

Previous studies demonstrated *FMO3* promoter activity in the HepG2 hepatocarcinoma cell line [13], but the endogenous *FMO3* gene is not expressed in these cells. The mechanism whereby *FMO3* is repressed in HepG2 cells has not been elucidated, but this knowledge would be informative regarding the suitability of this model system for continued studies on mechanisms controlling *FMO3* transcription.

To determine if the reduced levels of important liver-specific transcription factors [28] contribute to *FMO3* repression, expression vectors for C/EBPβ, HNF3β, and HNF4α were transiently expressed in HepG2 cells and relative FMO3 mRNA levels determined by quantitative RT-PCR DNA amplification (Fig. 2). No effect was observed with either C/EBPβ or HNF3β. However, HNF4α transient expression resulted in a 3.1-fold increase in FMO3 mRNA levels, suggesting that decreased HNF4α levels contribute to the absence of *FMO3* expression in these cells.

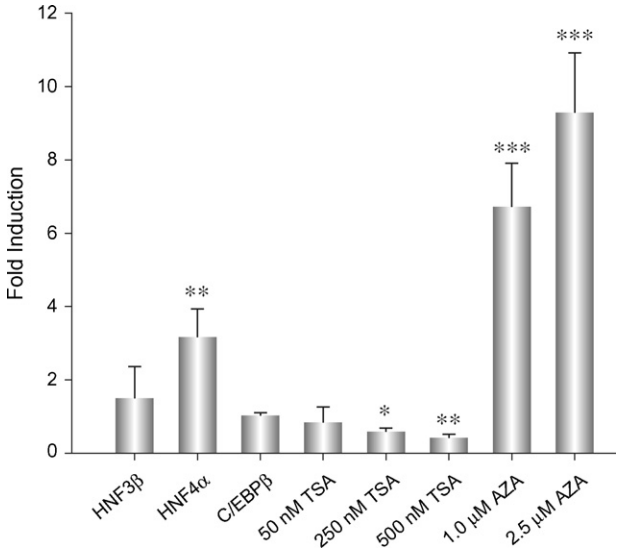

Fig. 2 – Factors effecting endogenous *FMO3* expression in HepG2 cells. HepG2 cells were transfected with 500 ng of HNF3β, HNF4α, or C/EBPβ expression vectors or treated with 50 nM, 250 nM, or 500 nM trichostatin A (TSA) for 24 h; or 1.0 μM or 2.5 μM 5-aza-2′-deoxycytidine (AZA) for 96 h. Following treatment, total RNA was isolated and GAPDH normalized FMO3 mRNA levels were determined by quantitative real-time RT-PCR. Data are expressed as the fold-change in expression relative to controls in which cells were transfected with empty expression vectors or treated with vehicle. Experimental and control ΔC_T values were compared using Student's t-test or one-way ANOVA with a Holm-Sidak post hoc test ($^{*}P < 0.05$, $^{**}P < 0.01$, and $^{***}P < 0.001$, respectively).

To investigate other potential mechanisms for *FMO3* repression, HepG2 cells were treated with trichostatin A to inhibit histone deacetylase or 5-aza-2′-deoxycytidine to inhibit DNA methyl transferase (Fig. 2). No changes in relative FMO3 mRNA levels were observed with 50 nM trichostatin A, while 250 nM or 500 nM trichostatin A treatments resulted in small but significant decreases in mRNA levels that were likely due to toxicity. These data suggest that histone acetylation plays a minimal role in repressing HepG2 cell *FMO3* expression. In contrast, 5-aza-2′-deoxycytidine at 1.0 μM and 2.5 μM resulted in 6.6- and 9.2-fold increases in FMO3 mRNA levels, respectively. Treatment with higher concentrations of 5-aza-2′-deoxycytidine also caused toxicity (data not shown). The observed increases in mRNA levels are consistent with DNA methylation being a major mechanism repressing HepG2 *FMO3* expression.

Three CpG sites are located within *FMO3* exon 1, and 31 are located within the first 4000-bps upstream of the transcription start site. Twenty of these latter sites are clustered within a region found at *FMO3* position −3899 to −3487. To determine whether methylation at one or more of these sites might contribute to *FMO3* repression, bisulfite DNA sequencing was performed between *FMO3* position −3999 and −3390 and position −279 and +440. No CpG methylation differences were observed between the bisulfite treated and untreated HepG2 DNA (data not shown). Nevertheless, the above experiments in total suggest that HepG2 cells, despite their limitations, are a suitable model for further exploring mechanisms regulating *FMO3* transcription using transient expression of reporter constructs, as there are no apparent defects in the transcriptional machinery necessary for expression at this locus.

Changes in methylation also have been implicated as a mechanism regulating the onset of hepatic drug metabolizing enzymes expression during development (*e.g.*, see [29]). As such, CpG methylation differences between *FMO3* position −3999 and −3390 and position −279 and +440 also were explored using DNA isolated from fetal and adult human liver. However, no differences were observed, suggesting hypermethylation is not playing a direct role in repressing *FMO3* in the fetal liver (data not shown).

3.2. *In vitro DNA–protein binding within FMO3 regulatory domain I*

Given the 3-fold increase in promoter activity associated with the *FMO3* domain I element (position −494 to −439) (Fig. 1) [13], initial EMSA experiments were conducted to identify specific protein interactions with these sequences. Using a DNA fragment representing *FMO3* position −500 to −475 as a probe (5′ portion of domain I) multiple, specific HepG2 DNA–protein complexes were observed. However, no specific DNA–protein interactions were observed with either fetal or adult liver nuclear protein extract (data not shown). As such, regulatory mechanisms involving these sequences were not pursued further. EMSA with a DNA fragment representing *FMO3* position −468 to −441 (3′ portion of domain I) identified several specific DNA–protein interactions, but also differential protein binding patterns among the three sources of nuclear

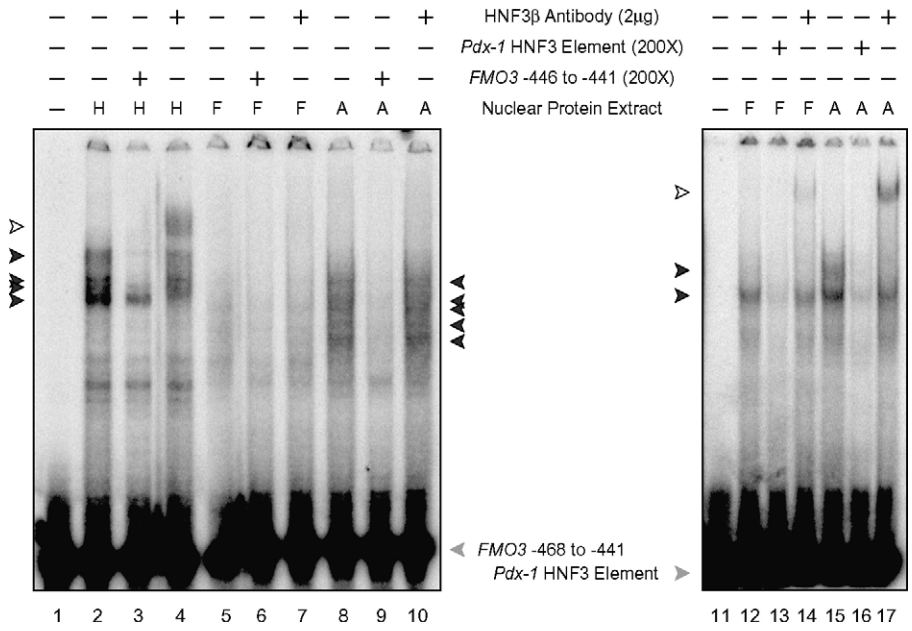

Fig. 3 – Developmental-specific *FMO3* DNA–proteins interactions. The sequence of the EMSA probes and the protocol followed are described under Section 2. Variables in each binding reaction are indicated above each lane (H = HepG2 cell; F = fetal liver; A = adult liver). Specific DNA–protein complexes are indicated by the solid arrows while unbound probe is indicated by the solid gray arrows. Supershifted complexes are indicated by the open arrows.

protein used in these experiments. Four specific DNA–protein complexes were observed with HepG2 nuclear protein extract (Fig. 3, lanes 2 and 3). In contrast, no specific DNA–protein complexes were observed with fetal liver nuclear protein extract (Fig. 3, lanes 5 and 6). Five specific DNA–protein complexes were observed with adult liver nuclear protein extract, three of which exhibited different mobilities compared to those observed with HepG2 nuclear proteins (Fig. 3, lanes 8 and 9).

Scanning the *FMO3* position −468 to −411 sequence against the TRANSFAC database identified a putative HNF3β recognition site with a core match of 1.0 and a matrix match of 0.913, and two overlapping putative C/EBP recognition sites with core matches of 1.000 and 0.986 and matrix matches of 0.775 and 0.898, respectively. Addition of HNF3β antibody to the EMSA binding reaction supershifted the major DNA–protein complex observed with HepG2 nuclear proteins (Fig. 3, lane 4), but had no effect on the DNA–protein complexes observed with adult liver nuclear proteins (Fig. 3, lane 10). To verify the presence of HNF3β in both the fetal liver and adult nuclear protein extract, a known HNF3β human *Pdx-1* promoter element [30] was used. A single specific DNA protein complex was observed with both nuclear protein extracts that was supershifted with the HNF3β antibody (Fig. 3, lanes 12–17).

Consistent with HNF3β present in HepG2 cell nuclear protein extract binding the *FMO3* domain I element, a single DNA–protein complex was eliminated by competition with an HNF3 consensus sequence (Fig. 4A, lanes 2–4). Furthermore, mutation of the core HNF3 binding site in the unlabeled probe, *FMO3* position −461 A > G, prevented self-competition (Fig. 4A, lane 5). In contrast, none of the DNA–protein complexes observed with adult liver nuclear proteins were eliminated by competition with the HNF3 consensus element (Fig. 4A, lane 10) and equal competition was observed with either the unchanged *FMO3* position −468 to −441 DNA fragment or this same fragment in which the HNF3 site was mutated (Fig. 4A, lane 11). Competition with a C/EBP consensus element eliminated all of the DNA–protein complexes observed with adult liver nuclear protein (Fig. 4A, lane 12) and all of the DNA–protein complexes observed with HepG2 cell nuclear proteins except for that previously identified as an HNF3β-DNA complex (Fig. 4A, lane 6). Mutation of the core C/EBP binding site, *FMO3* position −447 to −446 AA > TT, eliminated self-competition for all of the adult liver DNA–protein complexes (Fig. 4A, lane 13) and all of the HepG2 DNA–protein complexes, except for the previously identified HNF3β-DNA complex (Fig. 4A, lane 7). Thus, these data suggest independent, but overlapping binding elements for HNF3β and C/EBP within the 3′ half of the *FMO3* domain I element.

Given the existence of multiple C/EBP isoforms capable of recognizing similar DNA sequences, isoform specific antibodies were employed to identify the specific C/EBP family member(s) present in the nuclear protein extracts and capable of specifically binding the *FMO3* domain I element. C/EBPα and C/EBPβ, but not C/EBPγ or C/EBPδ antibodies supershifted at least one of the DNA–protein complexes using HepG2 nuclear protein extract (Fig. 4B, lanes 5–8). Inclusion of C/EBPα, C/EBPβ, or C/EBPδ, but not C/EBPγ antibodies in the EMSA binding reaction supershifted at least one of the DNA–protein complexes observed with adult liver nuclear protein extract (Fig. 4B, lanes 12–15). In both instances, the C/EBPβ antibody supershifted the greatest amount of the specific DNA–protein complexes.

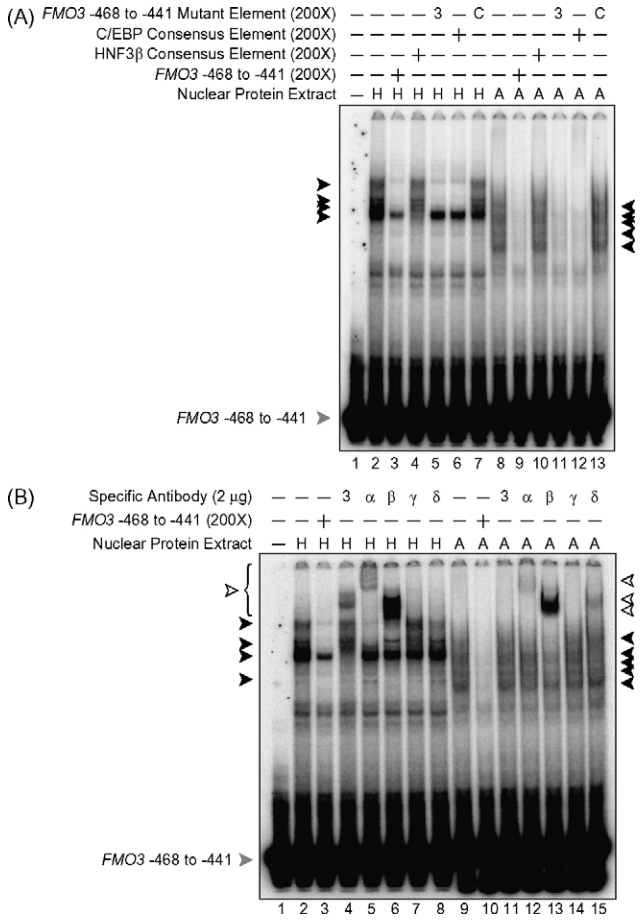

Fig. 4 – Identification of *FMO3* position −468 to −441 (domain I) specific DNA–protein interactions. The sequence of the EMSA probe and the protocol followed are described under Section 2. Variables in each binding reaction are indicated above each lane. In (A), H = HepG2 cell; A = adult liver; 3 = unlabeled *FMO3* −468 to −441 probe fragment containing the HNF3β element mutation, −461 A > G; and C = unlabeled *FMO3* −468 to −441 probe fragment containing the C/EBPβ element mutation, −447 to −446 AA > TT. In (B), H = HepG2 cell; A = adult liver; 3 = HNF3β antibody; α = C/EBPα antibody; β = C/EBPβ antibody; γ = C/EBPγ antibody; δ = C/EBPδ antibody. Specific DNA–protein complexes are indicated by the solid arrows while unbound probe is indicated by the solid gray arrows. Supershifted complexes are depicted by the open arrows.

3.3. *Functional analysis of the FMO3 HNF3, and C/EBP elements*

To determine the functional significance of the HNF3β and C/EBP *FMO3* promoter elements, the same mutations that eliminated transcription factor binding *in vitro*, *i.e.*, *FMO3* position −461A > G for HNF3β and position −447 to −446 AA > TT for C/EBP, were introduced into the pRNH694 *FMO3*/reporter construct, generating pRNH932 and pRNH968, respectively. These constructs were then tested for *FMO3* promoter activity by transient expression in HepG2 cells.

Co-transfecting HepG2 cells with increasing concentrations of the HNF3β expression vector and the pRNH694 *FMO3*/reporter construct failed to demonstrate any effect of HNF3β on *FMO3* promoter activity. Furthermore, comparing the transient expression of the pRNH694 and pRNH932 *FMO3*/reporter constructs revealed that mutating the HN3β element had no effect on promoter activity (data not shown). In contrast, co-transfection of HepG2 cells with the C/EBPβ expression vector and the pRNH694 reporter construct resulted in a dose-dependent increase in *FMO3* promoter activity with a maximal 2-fold increase using 1 μg of expression vector (data not shown). Subsequent experiments utilized 0.5 μg of expression vector to minimize potential over-expression artifacts. As seen in Fig. 5, co-transfection with 0.5 μg of the C/EBPβ expression vector and the pRNH694 *FMO3*/reporter construct resulted in a 1.5-fold increase in promoter activity. Similar experiments with C/EBPα or C/EBPδ expression vectors decreased promoter activity. Although a larger effect might be anticipated from a critical regulatory element, the HepG2 cells are known to express relatively high levels of endogenous C/EBPβ, thus tempering the effect size of these co-transfection studies. Consistent with an important regulatory role, transient expression of the pRNH968 *FMO3*/reporter construct (C/EBP site mutated) in HepG2 cells revealed a 55% reduction in promoter activity relative to pRNH694 (Fig. 5). The increased promoter activity observed after co-transfection with the C/EBPβ expression vector also was eliminated. However, neither the C/EBPα- nor C/EBPδ-dependent decreases in *FMO3* promoter activity were affected. Similar non-specific effects with both C/EBPα- and C/EBPδ transient expression were observed with *FMO3* promoter deletion constructs missing the domain I element and with the parent pGL3basic vector (data not shown). Taken together, these data suggest that HNF3β has minimal if any role in regulating *FMO3* promoter activity and that the effects observed with C/EBPα and C/EBPδ were due to secondary or non-specific squelching effects. In contrast, C/EBPβ appears to be a major factor regulating the *FMO3* promoter through the domain I element.

Multiple forms of C/EBPβ are known to exist due to the selection of alternative ATG start codons and/or proteolytic cleavage [31]. The dominant forms in liver are C/EBPβ LAP, a full-length or near full-length isoform, and C/EBPβ LIP, an N-terminal truncated form. A downstream ATG site is selected in the latter, eliminating all transactivation domains but retaining the DNA binding domain. Thus C/EBPβ LIP acts as a competitive repressor.

To further explore the role of C/EBPβ in regulating *FMO3* expression, HepG2 cells were transfected with *FMO3*/reporter constructs containing either the reference or mutated C/EBP site and different amounts of C/EBPβ LAP and/or C/EBPβ LIP expression vectors. To control for any non-specific effects, promoter activities for the pRNH694 (reference) *FMO3* reporter construct were normalized to the activities observed with pRNH968 (C/EBP site mutated) (Fig. 6). Co-expression with C/EBPβ LIP resulted in a dose-dependent decrease in *FMO3* promoter activity; the maximum decrease of 27% being observed with 50 ng of expression plasmid (Fig. 6). Increasing amounts of C/EBPβ LAP with a constant amount of C/EBPβ LIP reversed the inhibitory effect of the latter factor in a

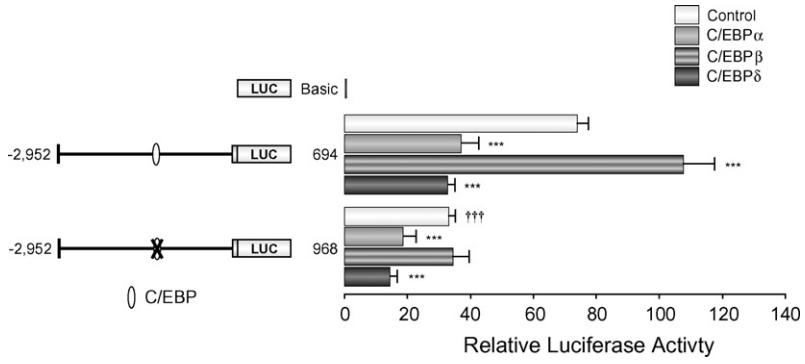

Fig. 5 – Functional analysis of *FMO3* C/EBP element. HepG2 cells were co-transfected with *FMO3*/luciferase reporter constructs containing either the mutated (AA > TT at position −447 to −446) or reference C/EBPβ element and 0.2 μg of the C/EBPα, C/EBPβ, C/EBPδ, or empty pBJ5 expression vectors. Salient features of each reporter construct as well as the plasmid identification number are shown on the left side of the bar graphs. Mutation of each regulatory element is indicated by an X. The activity reported has been normalized for transfection efficiency and represents the mean ± S.D. from a representative experiment that included four replicates for each transfection. The experiment was repeated a minimum of three times with similar results. Data were compared using one-way ANOVA with a Tukey post hoc test ($^{***}P < 0.001$ compared to the control expression plasmid; $^{\dagger\dagger\dagger}P < 0.001$ compared to reference construct).

dose-dependent fashion. At the highest concentration of C/EBPβ LAP, *FMO3* promoter activity was no different than that observed with LAP alone.

3.4. *Binding of C/EBPβ to the FMO3 promoter domain I element in intact cells and tissue*

ChIP was employed to determine whether or not C/EBPβ binding to the *FMO3* domain I element also would be observed in intact cells and tissue (Table 1). The well characterized C/EBPβ elements on both the albumin [21] and *CYP3A4* [22] genes were used as positive controls. In two independent experiments with primary human hepatocytes, significant differences in C_T values were observed, yielding a calculated 2.0- and 3.6-fold enrichment, respectively, of the *FMO3* C/EBP element due to C/EBPβ binding. A similar analysis of the albumin C/EBP element resulted in a 17.5- and 8.8-fold enrichment, while analysis of the *CYP3A4* C/EBP element resulted in a 7.5- and 11.8-fold enrichment, respectively. When these same ChIP experiments were repeated using pooled frozen human adult liver tissue, C/EBPβ binding resulted in a 2.1-fold enrichment for the *FMO3* element, a 3.9-fold enrichment for the albumin element, and a 7.3-fold enrichment for the *CYP3A4* element. No statistical differences in C_T were observed with the *FMO3* exon 9 or *GAPDH/CNAP1* intergenic negative control fragments in any of the experiments (data not shown).

3.5. *Evolutionary conservation of human FMO3 promoter elements*

Given the absence of hepatic *FMO3* expression in most mammalian species, *FMO3* gene sequences from multiple species were aligned to compare the critical human *FMO3* promoter elements identified to date ([13] and current study) (Fig. 7). Striking differences were observed. The *FMO3* proximal NFY CCAAT box element previously shown to be critical for constitutive expression was present in *Homo sapiens* and *Pan troglodytes*, but not *Macaca mulatta*, *Bos taurus*, *Canis lupus familiaris*, *Rattus norvegicus*, or *Mus musculus*. The Pbx_2/Hox, USF-1, YY1, and C/EBP elements identified on human *FMO3* are perfectly conserved in *P. troglodytes* and *M. mulatta*, except for a

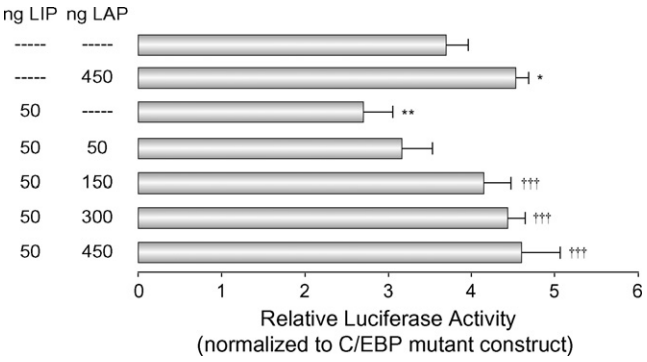

Fig. 6 – *FMO3* promoter regulation by the C/EBPβ LAP:LIP ratio. *FMO3*/luciferase reporter constructs (*FMO3* position −2952 to +42) containing either the mutated (position −447 to −446 AA > TT) or reference C/EBPβ element were transiently expressed in HepG2 cells along with different amounts of C/EBPβ LAP, C/EBPβ LIP, or empty pBJ5 expression vector. The amount of co-transfected expression vector is shown on the left side of the graph. The activity reported has been normalized for transfection efficiency and represents the mean ± S.D. from a representative experiment that included four replicates for each transfection. The experiment was repeated a minimum of three times with similar results. Transfection data for the reference constructs were normalized to the transfection data for the mutant constructs to illustrate the changes in promoter activity specific to the C/EBP element. Data were compared using one-way ANOVA with a Tukey post hoc test ($^{*}P < 0.05$ and $^{**}P < 0.01$, respectively, compared to the control transfection with the empty expression vector; $^{\dagger\dagger\dagger}P < 0.001$ compared to co-expression with pBJ-C/EBPβ LIP alone).

Table 1 – C/EBPβ binding to the *FMO3* domain I element in vivo

Gene	Expt. #	Source[a]	N[b]	C_T (mean ± S.D.)		ΔC_T	Fold enrichment[c]
				IgG	C/EBP		
CYP3A4	1	Hepatocytes	6	35.6 ± 0.7	32.6 ± 0.2[d]	3.0	7.5
	2	Hepatocytes	5	33.4 ± 0.6	29.7 ± 0.6[d]	3.7	11.8
	3	Tissue	5	34.7 ± 0.5	31.7 ± 0.4[d]	3.0	7.3
Albumin	1	Hepatocytes	4	34.3 ± 0.2	30.2 ± 0.3[d]	4.1	17.5
	2	Hepatocytes	5	31.5 ± 0.2	28.2 ± 0.3[d]	3.4	8.8
	3	Tissue	5	33.7 ± 0.9	31.6 ± 0.7[e]	2.1	3.9
FMO3	1	Hepatocytes	6	33.1 ± 0.7	32.0 ± 0.6[f]	1.1	2.0
	2	Hepatocytes	6	31.6 ± 0.7	29.7 ± 0.2[d]	2.0	3.6
	3	Tissue	6	32.7 ± 0.4	31.5 ± 0.4[d]	1.2	2.1

[a] Source of chromatin for ChIP reactions (see Section 2).
[b] Number of chromatin immunoprecipitation replicates.
[c] Calculated as (mean slope input DNA)$^{\Delta C_T}$.
[d] Significantly different than IgG control, unpaired *t*-test with Welch correction ($P < 0.001$).
[e] Significantly different than IgG control, unpaired *t*-test with Welch correction ($P < 0.05$).
[f] Significantly different than IgG control, unpaired *t*-test with Welch correction ($P < 0.01$).

single base change in both the *M. mulatta* USF-1 and YY1 elements. However, these single nucleotide changes would not appear to be functionally important based on an examination of the respective matrices in the TRANSFAC database. Also based on the TRANSFAC database matrices, *B. taurus FMO3* would appear to have functional YY1 and C/EBP elements and *Canis lupus familiaris FMO3* a functional C/EBP element, although sequences within all three elements are different than the respective elements in *H. sapiens* and *P. troglodytes*.

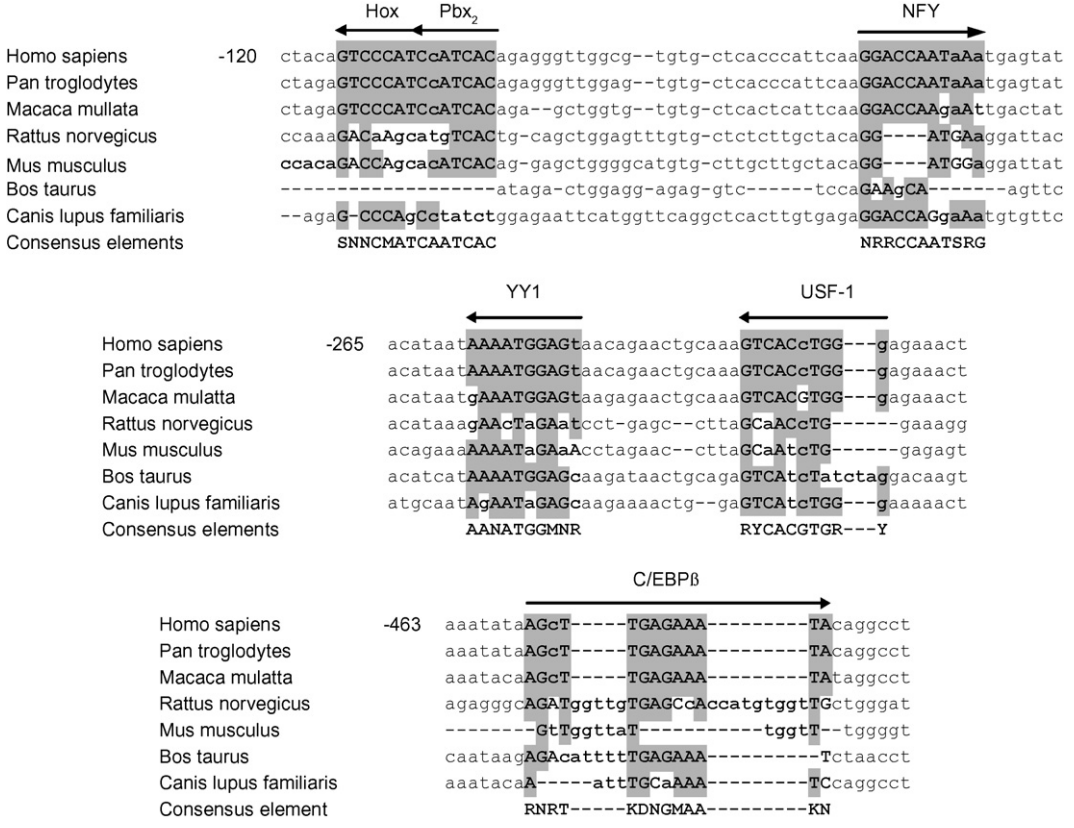

Fig. 7 – Sequence alignment of *FMO3* promoter elements. *FMO3* gene sequences from *Homo sapiens*, *Pan troglodytes*, *Macaca mullata*, *Rattus norvegicus*, *Mus Musculus*, *Bos taurus*, and *Canis lupus familiaris* were compared using an exhaustive pairwise global alignment algorithm and progressive assembly using Neighbor-Joining phylogeny. The shaded bases are conserved compared to the human gene, while upper case letters represent conserved bases compared to the consensus transcription factor binding matrix (TRANSFAC V11.1 database).

4. Discussion

There has been considerable controversy regarding the use of the HepG2 cell line as a model to elucidate mechanisms involved in liver-specific gene regulation. Although these cells express many liver-specific genes and exhibit characteristics typical of a normal hepatocyte phenotype [18], several drug metabolizing monooxygenases associated with the differentiated hepatic phenotype, including *FMO3*, are not expressed in these cells. Possible mechanisms underlying the absence of *FMO3* expression were explored in the current study. In contrast to what has been observed for several members of the cytochrome P450 family [22,28], endogenous HepG2 FMO3 mRNA levels were not increased by supplemented expression of the liver-specific transcription factors, C/EBPβ or HNF3β, suggesting the absence or deficiency of these factors is not limiting. A 3-fold increase in FMO3 mRNA levels was observed by transient expression of HNF4α in HepG2 cells. The absence of any responsive sites within the currently characterized *FMO3* promoter would argue for an indirect HNF4α regulatory mechanism. Although sites further upstream remain a possibility, none were identified by scanning against the TRANSFAC database.

Inhibiting DNA methyltransferase resulted in an approximate 10-fold increase in endogenous *FMO3* expression. Thus, DNA methylation appears to be a major mechanism responsible for silencing *FMO3* in HepG2 cells. Of interest, hypermethylation also has been shown to silence a number of other genes involved in xenobiotic disposition in HepG2 cells, *e.g.*, *ADH1B* and *1C* [32]. This mechanism might similarly function to repress *FMO3* expression in the human fetal liver. However, no differences in *FMO3* CpG site methylation were observed between fetal, adult and HepG2 cells. Differential methylation may still play a role in regulating *FMO3* developmental expression, as it does in repressing HepG2 *FMO3* expression, but likely does so through an indirect, rather than direct effect, *i.e.*, regulating the expression of one or more transcription factors important for *FMO3* expression. Most importantly for the current study, these observations suggest that HepG2 cells are an acceptable model for studying *FMO3* transcriptional regulation using transient expression of reporter constructs, as it appears *FMO3* repression in these cells is not due to an innate defect or deficiency in transcriptional machinery.

Of the *FMO3* regulatory domains characterized to date ([13] and current study), the C/EBP element within *FMO3* promoter domain I was the only one to display a distinct differential DNA–protein binding pattern in assays conducted with HepG2 cell, fetal and adult liver nuclear protein extract. Furthermore, mutation of this element reduced *FMO3* promoter activity by 55%, comparable to the reduction in promoter activity observed by mutagenesis of the more proximal NFY and Pbx_2/Hox *FMO3* regulatory elements [13]. None of these data would support synergism between any of these elements but do suggest that maximal *FMO3* constitutive expression requires the involvement of all three factors.

Human *FMO3* exhibits a highly specific tissue- and temporal-specific expression pattern. The C/EBPβ tissue- and temporal-specific expression pattern observed in rodent models is consistent with a role for C/EBPβ in contributing to the control of the *FMO3* human temporal- and tissue-specific expression pattern. Thus, despite the promiscuous expression of C/EBPβ mRNA, low C/EBPβ protein levels, if any, have been detected in extrahepatic tissues [33]. Similarly, low *FMO3* expression levels, if any, are observed in extrahepatic tissues [5]. Multiple studies in mice and rats also have shown low levels of C/EBPβ mRNA and protein in fetal liver but greatly increased levels in adult liver (*e.g.*, [34]). Assuming a similar pattern in the human, these data would explain the absence of C/EBPβ-*FMO3* domain I interactions using fetal liver nuclear protein. Furthermore, the C/EBPβ LAP:LIP ratio increases significantly during rat liver development, from about 3:1 before birth to 15:1 in adult rats, and exhibits a transient perinatal peak [34]. The observation that the C/EBPβ LAP:LIP ratio modulates *FMO3* promoter activity and assuming a similar change in the C/EBPβ LAP:LIP ratio during human hepatic development, such a change would be consistent with C/EBPβ contributing to the onset of *FMO3* expression in the perinatal period [7]. Interestingly, the C/EBPβ LAP:LIP ratio also was shown to have an even stronger influence on *CYP3A4* expression [22], a gene that exhibits a temporal-specific expression pattern in the liver similar to *FMO3* [35].

FMO3 also exhibits a pronounced species-specific expression pattern [5]. Of the mammals examined to date, only *H. sapiens*, *P. troglodytes*, and female *M. musculus* express FMO3 as the primary adult hepatic FMO enzyme [5,10,11]. Consistent with this observation, striking differences in key *FMO3* promoter elements were observed among several mammalian species. The proximal NFY CCAAT box element that is critical for human *FMO3* promoter function [13] was only conserved in *P. troglodytes*. The apparent absence of a functional NFY CCAAT box in the *M. mulatta FMO3* proximal promoter may explain why FMO1 and not FMO3 is the primary adult liver FMO enzyme in this species, despite all other critical human *FMO3* promoter elements identified to date being conserved. In contrast, other important human *FMO3* promoter elements are not conserved in further divergent mammals, *i.e.*, *B. taurus*, *Canis lupus familiaris*, *R. norvegicus*, and *M. musculus*. The lack of regulatory element conservation between *H. sapiens* and *M. musculus*, despite this enzyme being highly expressed in both male and female juvenile, as well as adult female *M. musculus*, suggests the gene is under very different regulatory mechanisms in these two species. Finally, the difference in *FMO3* expression between *P. troglodytes* and *M. mulatta* suggests a more recent evolutionary event resulting in FMO3 being expressed as the dominant hepatic FMO enzyme, and combined with the recent evidence for *FMO3* balanced selection [36], is suggestive of an important, but so far elusive FMO3 endogenous function.

In summary, this study extends a previous report in which *FMO3* regulatory domains within the first 2952-bps upstream of the transcription start site were characterized and important proximal transcription factor binding elements identified [13]. In the current report, a C/EBPβ element within the previously identified but uninvestigated more distal *FMO3* regulatory domain I (position −494 to −439) was characterized and shown to be important for regulating *FMO3* promoter activity. This same factor also may contribute to the previously characterized *FMO3* developmental expression pattern [7].

Acknowledgment

This work was supported in part by funds from the Children Research Institute, Children's Hospital and Health Systems.

Appendix A. Supplementary data

Supplementary data associated with this article can be found, in the online version, at doi:10.1016/j.bcp.2008.05.002.

REFERENCES

[1] Williams JA, Hyland R, Jones BC, Smith DA, Hurst S, Goosen TC, et al. Drug-drug interactions for UDP-glucuronosyltransferase substrates: a pharmacokinetic explanation for typically observed low exposure (AUCi/AUC) ratios. Drug Metab Dispos 2004;32:1201–8.
[2] Krueger SK, Williams DE. Mammalian flavin-containing monooxygenases: structure/function, genetic polymorphisms and role in drug metabolism. Pharmacol Ther 2005;106:357–87.
[3] Cashman JR, Zhang J. Human flavin-containing monooxygenases. Annu Rev Pharmacol Toxicol 2006;46:65–100.
[4] Hernandez D, Janmohamed A, Chandan P, Phillips IR, Shephard EA. Organization and evolution of the flavin-containing monooxygenase genes of human and mouse: identification of novel gene and pseudogene clusters. Pharmacogenetics 2004;14:117–30.
[5] Hines RN. Developmental and tissue-specific expression of human flavin-containing monooxygenase 1 and 3. Expert Opin Drug Metab Toxicol 2006;2:41–9.
[6] Hines RN, Hopp KA, Franco J, Saeian K, Begun FP. Alternative processing of the human hepatic *FMO6* gene renders transcripts incapable of encoding a functional flavin-containing monooxygenase. Mol Pharmacol 2002;62:320–5.
[7] Koukouritaki SB, Simpson P, Yeung CK, Rettie AE, Hines RN. Human hepatic flavin-containing monooxygenase 1 (*FMO1*) and 3 (*FMO3*) developmental expression. Pediatric Res 2002;51:236–43.
[8] Shimada T, Yamazaki H, Mimura M, Inui Y, Guengerich FP. Interindividual variations in human liver cytochrome P-450 enzymes involved in the oxidation of drugs, carcinogens and toxic chemicals: Studies with liver microsomes of 30 Japanese and 30 Caucasians. J Pharmacol Exp Ther 1994;270:414–23.
[9] Overby LH, Carver GC, Philpot RM. Quantitation and kinetic properties of hepatic microsomal and recombinant flavin-containing monooxygenases 3 and 5 from humans. Chem Biol Interact 1997;106:29–45.
[10] Stevens JC, Shipley LA, Cashman JR, Vandenbranden M, Wrighton SA. Comparison of human and rhesus monkey *in vitro* phase I and phase II hepatic drug metabolism activities. Drug Metab Dispos 1993;21:753–60.
[11] Rodrigues AD, Kukulka MJ, Ferrero JL, Cashman JR. In vitro hepatic metabolism of ABT-418 in chimpanzee (Pan troglodytes). A unique pattern of microsomal flavin-containing monooxygenase-dependent stereoselective N′-oxidation. Drug Metab Dispos 1995;23:1143–52.
[12] Zhang J, Cashman JR. Quantitative analysis of FMO gene mRNA levels in human tissues. Drug Metab Dispos 2006;34:19–26.
[13] Klick DE, Hines RN. Mechanisms regulating human *FMO3* transcription. Drug Metab Rev 2007;39:419–42.
[14] Hinokio Y, Horikawa Y, Furuta H, Cox NJ, Iwasaki N, Honda M, et al. Beta-cell transcription factors and diabetes: no evidence for diabetes-associated mutations in the hepatocyte nuclear factor-3beta gene (HNF3B) in Japanese patients with maturity-onset diabetes of the young. Diabetes 2000;49:302–5.
[15] Mendel DB, Hansen LP, Graves MK, Conley PB, Crabtree GR. HNF-1 alpha and HNF-1 beta (vHNF-1) share dimerization and homeo domains, but not activation domains, and form heterodimers in vitro. Genes Dev 1991;5:1042–56.
[16] Cereghini S. Liver-enriched transcription factors and hepatocyte differentiation. FASEB J 1996;10:267–82.
[17] Shadley JD, Divakaran K, Munson K, Hines RN, Douglas K, McCarver DG. Identification and functional analysis of a novel human *CYP2E1* far upstream enhancer. Mol Pharmacol 2007;71:1630–9.
[18] Aden DP, Fogel A, Plotkin S, Damjanov I, Knowles BB. Controlled synthesis of HBsAg in a differentiated human liver carcinoma-derived cell line. Nature 1979;282:615–6.
[19] Luo Z, Hines RN. Identification of multiple flavin-containing monooxygenase form 1 (*FMO1*) gene promoters and observation of tissue-specific DNaseI hypersensitive sites. Arch Biochem Biophys 1996;336:251–60.
[20] Bookout AL, Cummins CL, Kramer MF, Pesola JM, Mangelsdorf DJ. High-throughput real-time quantitative reverse transcriptase PCR. In: Ausubel FM, Brent R, Kingston RE, Moore DD, Seidman JG, Smith JA, Struhl K, editors. Current protocols in molecular biology. New York: John Wiley & Sons; 2006. p. 15.8.1–28.
[21] Trautwein C, Rakemann T, Pietrangelo A, Plumpe J, Montosi G, Manns MP. C/EBP-beta/LAP controls down-regulation of albumin gene transcription during liver regeneration. J Biol Chem 1996;271:22262–70.
[22] Martinez-Jimenez CP, Gomez-Lechon MJ, Castell JV, Jover R. Transcriptional regulation of the human hepatic CYP3A4: identification of a new distal enhancer region responsive to CCAAT/enhancer-binding protein beta isoforms (liver activating protein and liver inhibitory protein). Mol Pharmacol 2005;67:2088–101.
[23] Aparicio O, Geisberg JV, Sekinger e, Yang A, Moqtaderi Z, Struhl K. Chromatin immunoprecipitation for determining the association of proteins with specific genomic sequences in vivo. In: Ausubel FM, Brent R, Kingston RE, Moore DE, Seidman JG, Smith JA, Struhl K, editors. Current protocols in molecular biology. New York: John Wiley & Sons; 2005. p. 21.3.1–30.
[24] Li LC, Dahiya R. MethPrimer: designing primers for methylation PCRs. Bioinformatics 2002;18:1427–31.
[25] Koukouritaki SB, Poch MT, Cabacungan ET, McCarver DG, Hines RN. Discovery of novel flavin-containing monooxygenase 3 (*FMO3*) single nucleotide polymorphisms and functional analysis of upstream haplotype variants. Mol Pharmacol 2005;68:383–92.
[26] Matys V, Kel-Margoulis OV, Fricke E, Liebich I, Land S, Barre-Dirrie A, et al. TRANSFAC and its module TRANSCompel: transcriptional gene regulation in eukaryotes. Nucleic Acids Res 2006;34:D108–10.
[27] Kel AE, Gossling E, Reuter I, Cheremushkin E, Kel-Margoulis OV, Wingender E. MATCH: a tool for searching transcription factor binding sites in DNA sequences. Nucleic Acids Res 2003;31:3576–9.
[28] Jover R, Bort R, Gómez-Lechón MJ, Castell JV. Re-expression of C/EBPa induces CYP2B6, CYP2C9 and CYP2D6 genes in HepG2 cells. FEBS Lett 1998;431:227–30.
[29] Vieira I, Sonnier M, Cresteil T. Developmental expression of *CYP2E1* in the human liver. Hypermethylation control of

gene expression during the neonatal period. Eur J Biochem 1996;238:476–83.
[30] Gerrish K, Gannon M, Shih D, Henderson E, Stoffel M, Wright CV, et al. Pancreatic beta cell-specific transcription of the pdx-1 gene. The role of conserved upstream control regions and their hepatic nuclear factor 3beta sites. J Biol Chem 2000;275:3485–92.
[31] Schrem H, Klempnauer J, Borlak J. Liver-enriched transcription factors in liver function and development. Part II: the C/EBPs and D site-binding protein in cell cycle control, carcinogenesis, circadian gene regulation, liver regeneration, apoptosis, and liver-specific gene regulation. Pharmacol Rev 2004;56: 291–330.
[32] Dannenberg LO, Chen HJ, Tian H, Edenberg HJ. Differential regulation of the alcohol dehydrogenase 1B (*ADH1B*) and *ADH1C* genes by DNA methylation and histone deacetylation. Alcohol Clin Exp Res 2006;30:928–37.
[33] Descombes P, Chojkier M, Lichtsteiner S, Falvey E, Schibler U. LAP, a novel member of the C/EBP gene family, encodes a liver-enriched transcriptional activator protein. Genes Dev 1990;4:1541–51.
[34] Descombes P, Schibler U. A liver-enriched transcriptional activator protein, LAP, and a transcriptional inhibitory protein, LIP, are translated from the same mRNA. Cell 1991;67:569–79.
[35] Hines RN. Ontogeny of drug metabolism enzymes and implications for adverse drug reactions. Pharamcol Therapeut 2008;118:250–67.
[36] Allerston CK, Shimizu M, Fujieda M, Shephard EA, Yamazaki H, Phillips IR. Molecular evolution and balancing selection in the flavin-containing monooxygenase 3 gene (FMO3). Pharmacogenet Genomics 2007;17:827–39.